JACS
JOURNAL OF THE AMERICAN CHEMICAL SOCIETY

Article

pubs.acs.org/JACS

Tailoring the Chain Packing in Ultrathin Polyelectrolyte Films Formed by Sequential Adsorption: Nanoscale Probing by Positron Annihilation Spectroscopy

John F. Quinn,[†] Steven J. Pas,[‡,§] Anthony Quinn,[†] Heng Pho Yap,[†] Ryoichi Suzuki,[∥] Filip Tuomisto,[⊥] Bijan S. Shekibi,[‡,§] James I. Mardel,[‡] Anita J. Hill,*[,‡,§] and Frank Caruso*[,†]

[†]Department of Chemical and Biomolecular Engineering, The University of Melbourne, Victoria 3010, Australia

[‡]CSIRO Materials Science and Engineering and CSIRO Process Science and Engineering, Private Bag 33, Clayton South, Victoria 3169, Australia

[§]ARC Centre of Excellence for Electromaterials Science, School of Chemistry and Department of Materials Engineering, Monash University, Clayton, Victoria 3800, Australia

[∥]Advanced Defect Characterization Group, National Institute of Advanced Industrial Science and Technology, AIST, Tsukuba Central 2, Tsukuba, Ibaraki 305-8568, Japan

[⊥]Department of Applied Physics, Aalto University, POB 11100, FI-00076 Aalto, Finland

Supporting Information

ABSTRACT: Depth profiling experiments by positron annihilation spectroscopy have been used to investigate the free volume element size and concentration in films assembled using the layer-by-layer (LbL) adsorption method. Films prepared from strong polyelectrolytes, weak polyelectrolytes, hydrogen-bonding polymers, and blended polyelectrolyte multilayers have different chain packing that is reflected in the free volume characteristics. The influence of various parameters on free volume, such as number of bilayers, salt concentration, solution pH, and molecular weight, has been systematically studied. The free volume cavity diameters vary from 4 to 6 Å, and the free volume concentrations vary from (1.1−4.3) × 10^{20} cm^{-3}, depending on the choice of assembly polymers and conditions. Films assembled from strong polyelectrolytes have fewer free volume cavities with a larger average size than films prepared from weak polyelectrolytes. Blending the weak polyanion poly(acrylic acid), PAA, with the strong polyanion poly(styrene sulfonate), PSS, to layer alternately with the polycation poly(allyamine hydrochloride), PAH, is shown to be a viable method to achieve intermediate free volume characteristics in these LbL films. An increase in salt concentration of the adsorption solutions for films prepared from strong polyelectrolytes makes these films tend toward weaker polyelectrolyte free volume characteristics. Hydrogen-bonded layered films show larger free volume element size and concentration than do their electrostatically bonded counterparts, while reducing the molecular weight of these hydrogen-bonded polymers results in slightly reduced free volume size and concentration. A study of the effect of solution pH on films prepared from weak polyelectrolytes shows that when both polyelectrolytes are substantially charged in solution (assembly pH = 7.5), the chains pack similarly to strong polyelectrolytes (i.e., lower free volume concentration), but with smaller average cavity sizes. These results give, for the first time, a clear indication of how the free volume profile develops in LbL thin films, offering numerous methods to tailor the Ångström-scale free volume properties by judicious selection of the assembly polymers and conditions. These findings can be potentially exploited to tailor the properties of thin polymer films for applications spanning membranes, sensing, and drug delivery.

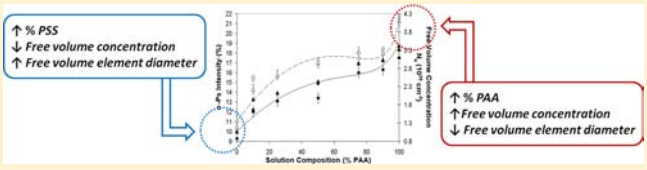

The preparation of thin films with controlled properties is important in a plethora of areas, including biomaterials, membranes, optics, and catalysis. For instance, a thin film coating can be used to alter the transport properties of a membrane,[1] the optical properties of a lens,[2] the catalytic performance of a supported catalyst,[3] or the biocompatibility of an implantable material.[4] Recently, there has been considerable interest in techniques that allow the manipulation of thin film coatings on very small thickness scales, particularly in the sub-100 nm range. One technique that has received widespread interest is the layer-by-layer (LbL) technique,[5,6] which involves the sequential adsorption of complementary species onto a surface. One of the main advantages of the LbL approach is its versatility: a vast number of different materials have been used.[5−15] While initial work in the area focused on complementary polymer systems (such as positively and negatively charged polyelectrolytes,[5,6] or polymers with hydrogen-bonding donor and acceptor groups[7,8]), the technique has

Received: September 2, 2012
Published: November 21, 2012

dx.doi.org/10.1021/ja308716v | J. Am. Chem. Soc. 2012, 134, 19808−19819

been extended to systems wherein a polymer is assembled alternately with a biomolecule (such as a protein,[9] an enzyme,[10] or a polynucleotide[11]), or with inorganic species such as metal[12] or metal oxide[13] nanoparticles. Films have also been assembled in which both species are biomolecules,[14] and even in which both species are nanoparticles.[15] These advances have demonstrated the scope of surface modification possible with the LbL approach and the variety of different surface chemistries that may be achieved. Further, the ability to vary the film thickness through altering the number of adsorbed layers (or the specific adsorption conditions) means that films of a wide range of thicknesses can be readily prepared. Such control of the film properties is difficult to achieve through other approaches, such as surface grafting or monolayer assembly.

One of the challenges of exploring films with nanoscale dimensions is that of thorough characterization. Ellipsometry,[16] surface plasmon resonance spectroscopy,[17] optical waveguide light spectroscopy,[18] and quartz crystal microgravimetry[19] have all been used for determining film thickness, while atomic force microscopy[20] and transmission electron microscopy[21] have provided information regarding film morphology and topography. Dynamic mechanical analysis[22,23] and differential scanning calorimetry[24] have also been used for examining the mechanical and thermal properties of films, but application of these approaches has been restricted to situations where a substantial amount of film material is present. The conformations of the polymer chains in the film have also been investigated using infrared spectroscopy[25] (particularly in the case of films incorporating polypeptides) or with nuclear magnetic resonance spectroscopy.[26,27] One area of particular importance in many thin film applications is the porosity of the films, in particular both the number and the size of the free volume elements. To this end, we have explored the use of positron annihilation spectroscopy (PAS) techniques[28−31] to investigate the concentration and size of free volume in thin films prepared using the LbL technique. PAS techniques have been used to measure the Ångström-scale free volume and thereby predict molecular and ionic transport properties in barrier and membrane polymers, and polymer electrolytes.[31−34] Hao et al. first reported the application of positrons to measure film thicknesses of polyelectrolyte/nanoparticle multilayer films;[35] however, this study was essentially confined to an analysis of film thickness.

Studies on the internal structure of polyelectrolyte multilayers, and in particular multilayer porosity, have been reviewed by Schönhoff et al.[36] Within the studies undertaken, attempts to probe the nanoscale porosity of polyelectrolyte multilayers have been rare. Vaca Chavez and Schönhoff used nuclear magnetic resonance cryoporometry to investigate nanoscale porosity in poly(allylamine hydrochloride) (PAH)/poly(sodium 4-styrenesulfonate) (PSS) multilayers.[37] NMR cryoporometry relies on the fact that crystals entrapped in a porous structure melt at a lower temperature than those in the bulk liquid. To perform NMR cryoporometry, a sample is first saturated with a suitable liquid and cooled until all of the liquid is frozen. Thereafter the sample is heated, resulting in melting of the liquid in the smallest pores first. Therefore, the evolution of an NMR signal with increasing temperature can be used to estimate the pore size distribution. It was demonstrated that this approach can be used to estimate the porosity in a number of PAH/PSS multilayer films formed on colloidal silica, and observed pore sizes in the range of 1 nm were reported.[37] A slight dependence with layer number was noted, with higher layer numbers resulting in slightly larger pores.

Pore size distributions in multilayer films have also been investigated using permeation approaches. For instance, Liu and Bruening have investigated the pore sizes in PAH/PSS multilayers by examining the transport of a number of neutral molecules through multilayer films supported on porous alumina substrates.[38] By modeling solute and solvent fluxes and rejection values for molecules of varying Stokes radii, these authors were able to estimate a pore radius for PAH/PSS multilayers in the order of 0.4−0.5 nm (i.e., a diameter of 0.8−1.0 nm). Other investigations by Jin et al., using a different substrate and suite of probe molecules, yielded a similar pore diameter of 0.67 nm for PAH/PSS multilayers.[39] These data are in good agreement with those obtained by NMR cryoporometry.

Variations in film density on much larger length scales have also been noted. Pulsed field gradient nuclear magnetic resonance spectroscopy (PFG-NMR) was employed by Wende and Schönhoff to investigate diffusion of water in polyelectrolyte multilayers of PSS and poly(diallyldimethylammonium chloride).[40] Measurements suggested that water molecules underwent restricted diffusion in a porous structure: however, the computed pore size using a model of restricted diffusion was shown to be in the order of micrometers. Following correction for the effect of cross relaxation rates, it was demonstrated that there was an observed pore size in the order of 4 μm. This result was interpreted as the presence of domains having lower polymer density and therefore faster water diffusion. These results show that porosity in polyelectrolyte multilayers may be observed on substantially differing length scales, and can be significantly influenced by factors such as layer number and preparation conditions (such as the presence of supporting electrolyte in the adsorption solutions). Given the limited number of studies on porosity in multilayer films, there is scope for an extensive study that examines films of varying chemical composition, such as those prepared under a variety of assembly conditions.

Herein, we present a comprehensive study of a range of LbL films using PAS. In particular, we examine the effect on the free volume element size and concentration in LbL-assembled films of varying (i) polymeric composition, (ii) adsorbed layer number, (iii) ionic strength of the adsorption solutions, (iv) molecular weight of the adsorbed polymeric species, and (v) pH of the adsorption solutions. We demonstrate that PAS can elucidate the free volume properties of LbL thin films. Moreover, we show that by varying film assembly conditions and components, it is possible to tailor the nanostructure of LbL films. Data derived from PAS will enable the preparation of films with tailored free volume and transport properties.[31]

MATERIALS AND METHODS

Materials. Poly(allylamine hydrochloride) (PAH, M_w = 70 000 g mol^{-1}), poly(acrylic acid, sodium salt) (PAA, M_w = 30 000 g mol^{-1}), poly(styrene sulfonate, sodium salt) (PSS, M_w = 70 000 g mol^{-1}), poly(*N*-vinyl pyrrolidone) (PVP, M_w = 10 000 or 360 000 g mol^{-1}), and poly(ethyleneimine) (PEI, M_w = 20 000 g mol^{-1}, water free) were obtained from Sigma-Aldrich and used without further purification. Poly(methacrylic acid) (PMA, M_w = 15 000 or 100 000 g mol^{-1}) was obtained from Polysciences Inc. Sodium chloride, hydrochloric acid, and sodium hydroxide were purchased from BDH and used as received. Oxidized monocrystalline silicon wafers were obtained from MMRC Pty. Ltd. (Melbourne, Australia). An inline Millipore RiOs/

Table 1. LbL Films: Polymer Composition, Assembly pH, [NaCl], Bilayer Number, and Film Thickness

polymer A	assembly pH A[a]	polymer B	assembly pH B[a]	[NaCl]	bilayer no.	film thickness (nm) t (nm) AFM[b]	film thickness (nm) t (nm) ellips[c]	t (nm) PAS	Figure ID
90%PSS/10%PAA	3.5	PAH	7.5	0	20[d]			85	1
75%PSS/25%PAA	3.5	PAH	7.5	0	20[d]			131	1
50%PSS/50%PAA	3.5	PAH	7.5	0	20[d]			191	1
25%PSS/75%PAA	3.5	PAH	7.5	0	20[d]			227	1
10%PSS/90%PAA	3.5	PAH	7.5	0	20[d]			271	1
PAA	3.5	PAH	7.5	0	20[d]			560	1
PSS	3.5	PAH	7.5	0	50[e]		120	123	2,3
90%PSS/10%PAA	3.5	PAH	7.5	0	20	150	139	131	2,3
75%PSS/25%PAA	3.5	PAH	7.5	0	20		154	170	2,3
50%PSS/50%PAA	3.5	PAH	7.5	0	20[e]		255	255	2,3
25%PSS/75%PAA	3.5	PAH	7.5	0	20		337[f]	380	2,3
10%PSS/90%PAA	3.5	PAH	7.5	0	20		587[g]	–	2,3
PAA	3.5	PAH	7.5	0	10		594	507	2,3
75%PSS/25%PAA	3.5	PAH	7.5	0	10[d]		51	53	2,3
50%PSS/50%PAA	3.5	PAH	7.5	0	10[d]		88	88	2,3
25%PSS/75%PAA	3.5	PAH	7.5	0	10[d]		87	88	2,3
10%PSS/90%PAA	3.5	PAH	7.5	0	10[d]		124	146	2,3
90%PSS/10%PAA	3.5	PAH	7.5	0	10[d]		41	53	5,7
90%PSS/10%PAA	3.5	PAH	7.5	0	15[d]		78	78	5,7
90%PSS/10%PAA	3.5	PAH	7.5	0	20	150	139	131	5,7
90%PSS/10%PAA	3.5	PAH	7.5	0	40	323	322	322	5,7
90%PSS/10%PAA	3.5	PAH	7.5	0	60	611	517	594	5,7
PSS	–	PAH	–	0.5	25	71	76	84	6,7
PSS	–	PAH	–	0.1	50		100	109	6,7
PSS	–	PAH	–	0.5	50	154	160	178	6,7
PSS	–	PAH	–	0.5	75	241	237	242	6,7
PSS	–	PAH	–	0.01	50		46	48	8
PSS	–	PAH	–	0.1	50		100	109	8
PSS	–	PAH	–	0.5	50	154	160	165	8
PSS	–	PAH	–	1	50	–	206	232	8
PSS	–	PAH	–	2	50	–	284	320	8
PMA (M_w = 100 kDa)	5.0	PVPON (M_w = 360 kDa)	5.0	0	40	–	145	150	9
PMA (M_w = 15 kDa)	5.0	PVPON (M_w = 10 kDa)	5.0	0	40	–	100	107	9
PAA	7.5	PAH	7.5	0	20	100	–	88	10
PAA	3.5	PAH	3.5	0	20	–	102	131	10
PAA	3.5	PAH	7.5	0	10	–	594	507	10
PAA	3.5	PAH	7.5	0	20	2000[h]	–	3000	10

[a]Dash indicates that the pH was not adjusted after preparing a 1 mg mL^{-1} solution of the polymer at the indicated sodium chloride concentration. [b]Thickness determined by abrading the film surface and measuring the height profile between the film surface and substrate. [c]Thickness determined from spectroscopic ellipsometry data using a classical wavelength dispersion model. [d]Films prepared by manual deposition without agitation of samples during adsorption or rinsing. [e]Cross-sectional scanning electron microscopy images for these samples are provided in the Supporting Information (Figure S1). [f]There was a thickness gradient evident across the sample. The value given is the average between the thicknesses on either edge of the sample (325–349 nm). [g]There was a thickness gradient evident across the sample. The value given is the average between the thicknesses on either edge of the sample (569–605 nm). [h]The sample was very rough, and the reported thickness represents an approximate average.

Origin system was used to produce high-purity water with a resistivity greater than 18 MΩ cm.

Substrate Preparation. Silicon wafers were cleaned and hydrophilized via the RCA protocol. The wafers were first sonicated in a 1:1 mixture of water and isopropanol for 15 min, followed by extensive rinsing in water. Thereafter, the wafers were heated at 60 °C for 15 min in a 5:1:1 mixture of water, hydrogen peroxide (30%), and ammonia solution (29%). The wafers were then again rinsed in purified water and stored under water until use.

Preparation of Multilayer Films. Stock polyelectrolyte solutions (2 mg mL^{-1}) were prepared and used to make up adsorption solutions at a final polyelectrolyte concentration of 1 mg mL^{-1}. A stock solution of sodium chloride (4 M) was also prepared and an appropriate amount added where sodium chloride was required in the final adsorption solution. The pH of the adsorption solutions was adjusted using 1 M NaOH and 1 M HCl where required. The polyanion solutions were adjusted to a pH of 3.5 or 7.5, and the PAH solutions were prepared to pH 3.5 or 7.5. The pH assembly conditions for each film are indicated in Table 1 and in the text. A precursor layer of PEI (1 mg mL^{-1}, 0.5 M NaCl) was always deposited as the first layer. Thereafter, the films were assembled using a Nanostrata Stratosequence automated dipcoater,[41,42] employing a 15 min adsorption time for the polyelectrolyte and 3 × 1 min water rinses (all with substrate spinning) for each deposition step. The films were gently blow-dried with nitrogen after each layer. In some cases, samples were prepared manually rather than automated deposition (this is indicated in Table 1).

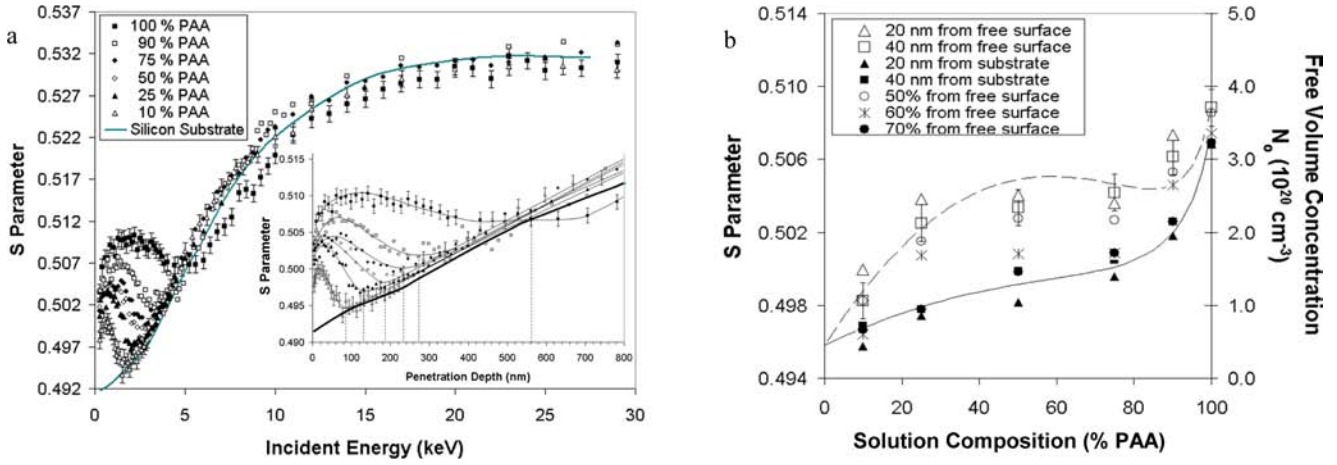

Figure 1. (a) Doppler broadening S parameter as a function of incident energy and penetration depth (inset). Vertical lines in inset indicate film thickness. The thick line is the silicon substrate. (b) Doppler broadening S parameter data and free volume concentration as a function of adsorption solution composition and depth. Lines are Kwei interaction parameter fits[60] (k = 10.72 and q increases from 0.0094 to 0.0320 to accurately model near-substrate versus near-free surface data, respectively). Films were prepared by manual deposition.

Atomic Force Microscopy (AFM) – Planar Films. AFM images were taken on air-dried films with a Nanoscope IIIa microscope and a MFP-3D Asylum Research instrument in noncontact mode using silicon cantilevers with a resonance frequency of ca. 290 kHz (Budget Sensors BSTop300). Image processing (first-order flattening and plane fitting) was carried out with Nanoscope 4.43r8 and Igor Pro 5.04B for images acquired using the Nanoscope IIIa and MFP-3D, respectively. To measure the film thickness, a scalpel blade was used to abrade the films in several areas, and images were taken at several points across the edge of each abrasion. The horizontal distance between two peaks in the height distribution analysis was determined as the film thickness.

Spectroscopic Ellipsometry. Measurements were performed on a UVISEL model ellipsometer from Horiba Jobin Yvon. Spectroscopic data were acquired between 340 and 825 nm with a 5 nm increment, and thicknesses were extracted with the integrated software by fitting with a classical wavelength dispersion model.[43] Reference optical parameters, as provided by Horiba from published reference data, were used for the silicon and silicon oxide layers of the substrate. The classical Drude–Lorentz model was used as the dispersion model for the polyelectrolyte multilayers. Being a dispersion model, no optical constants were assumed, as the material optical properties are wavelength dependent. A blank silicon substrate was measured in each instance to ensure the silicon oxide layer thickness was within reasonable expectation (~2.4 nm), and then the ellipsometric data were fitted to extract the polyelectrolyte film thickness.

Positron Annihilation Spectroscopy. The positron experiments were performed using two well-established beams, one at Aalto University[29] to measure Doppler broadening S parameter and one at AIST Tsukuba[28,30] to measure positron lifetimes and intensities. The Doppler broadening spectroscopy technique measures the momentum distribution of the annihilation photons and assigns the low momentum fraction, the S parameter, to positronium (Ps). When Ps is formed, about one-quarter of its intensity is paraPositronium and about three-quarters is orthoPositronium. Positron annihilation lifetime spectroscopy uses orthoPositronium (oPs) to determine the size and number of free volume elements in the polymer film. Prior to annihilation, oPs will localize in free volume elements. As the free volume element gets larger, the oPs lifetime increases; hence, the oPs lifetime reflects the size of the free volume element. The free volume element diameter is calculated using the Tao–Eldrup formula.[44,45] The number of positrons annihilating as oPs, as determined by the intensity parameter, yields information on the concentration of free volume elements. The concentration of free volume elements, N_o, was calculated using a value of trapping probability by range of 1 nm[46] and a linear relationship between S parameter and oPs intensity.[28,47] The relationship between the S parameter and oPs intensity for the LbL blends in this work has a linear regression coefficient R^2 of 0.77. oPs has a diffusion length of approximately 1–2 nm in polymers. Peak implantation depth was calculated using the Makhov–Baker power-law profile for positrons.[48,49] The mean implantation depth, $z_{1/2}$, is calculated as $z_{1/2} = 40(E^{1.6})/\rho$, where $z_{1/2}$ has units of nm, E has units of keV, and the density of the polyelectrolyte multilayer, ρ, is 1.0 ± 0.1 g/cm^3.[50] A good check of the reliability of the calculation is a comparison of film thickness as determined by oPs annihilation characteristics and ellipsometry; in all cases for this work, both techniques give values that agree within 20%, with the values for the majority of films differing by <5% (see Table 1). At low incident energies, <0.65 keV, the oPs formed in the near-surface region escapes from the surface into the vacuum, and for this condition the data analysis is less reliable for extraction of the oPs component in the thin film.[28] As discussed in the text, the standard deviation on the oPs lifetime component gives a good indication of when oPs annihilations in the thin film are reliably fitted; hence, due to unreliability, low incident energy data (<0.65 keV) for oPs lifetime and free volume element size are not presented. The contribution to the background from backscattered positrons at the sample surface is accounted for by using kapton film as a reference for the background.[28]

RESULTS AND DISCUSSION

Blends. A number of studies have demonstrated that preparing multilayer films, in which one of the adsorption steps involves the coadsorption of two or more species, can lead to films with enhanced properties, such as film stability,[51] composition,[52,53] and pH response.[54] Previous studies have shown that by having two polyelectrolytes in one of the adsorption solutions, it is possible to obtain film properties that are intermediate between the films prepared using only a single polyelectrolyte in the adsorption solution.[51−58] For instance, films prepared from blended polyanion solutions of PAA and PSS have thicknesses[54,57] and compositions[53,58] that fall between films assembled from the respective single polyelectrolytes. Further, films that are prepared from this polyanion blend, adsorbed in alternation with PAH, also have protein adsorption characteristics that are between the values obtained when only PAA or PSS is used as the polyanion.[53] Hence, studies were undertaken to investigate the material properties of films prepared from PAH adsorbed in alternation with a blend of PSS and PAA. Detailed characterization of the PAH-PSS/PAA blend films, including growth profiles by ellipsometry, quartz crystal microgravimetry, X-ray photoelectron

dx.doi.org/10.1021/ja308716v | J. Am. Chem. Soc. 2012, 134, 19808−19819

spectroscopy, fluorescence, and contact angle measurements, and film topography by AFM, can be found in our earlier publications.[53,54,57]

Figure 1a shows the Doppler broadening spectroscopy results for these films deposited on a silicon substrate. At low energies, the oPs, which is the free volume probe, is near the free surface; for example, an implantation energy of 0.65 keV gives a penetration depth of 20 nm. Higher energies give greater penetration depth into the film until the implantation depth is greater than the film thickness; at that point, Doppler broadening spectroscopy results are indicative of the silicon substrate. In Figure 1a, the *S* parameter values for the silicon substrate are shown as a solid line. The inset of Figure 1a shows the *S* parameter data as functions of positron penetration depth. Film thicknesses determined by Doppler broadening spectroscopy are marked by dashed vertical lines in Figure 1a (inset) and coincide with the minima as the data for the thin films overlay the silicon substrate line. Figure 1a shows that the PAA-rich films are thicker and have larger *S* parameters than do the PAA-lean films. The data in Figure 1a can be examined as a function of both implantation depth and adsorption solution composition, as shown in Figure 1b. As noted in our earlier studies on films assembled from polyanion blends of PAA and PSS, an increasing proportion of PAA in the adsorption solution leads to a commensurate increase in the amount of PAA in the film prepared.[53,54]

The *S* parameter is related to the fraction of oPs, the free volume probe, and can be expressed as the concentration of free volume elements, N_o (see Materials and Methods). Figure 1b shows the *S* parameter and concentration of free volume near the free surface and near the substrate in the LbL films as a function of adsorption solution composition. The free volume concentration varies with blend composition with the blends intermediate. There is a gradient in free volume concentration across the film thickness with the near-surface material having a greater number of free volume elements than the near-substrate material. The variation of free volume concentration with composition differs between near-surface material and near-substrate material, displaying S-shaped behavior near the free surface.

S-shaped compositional behavior in bulk polymer blends has been attributed to phase heterogeneity and quantified in terms of interaction parameters between the polymers.[59] The Kwei model[59−61] is used to determine two constants, k and q, that give information on the contribution to blend properties from additive volume or entropy mixing (k) or from heterogeneous specific interactions (q). The Kwei equation can be expressed as:

$$P = \frac{w_1 p_1 + w_2 p_2}{w_1 + k w_2} + q w_1 w_2 \quad (1)$$

where P is the blend property, w_1 is the weight fraction of component 1, p_1 is the property of component 1, w_2 is the weight fraction of component 2, and p_2 is the property of component 2. The Kwei model fits for the data in Figure 1b (dotted and solid lines) can be used to quantitatively distinguish the near free surface and near substrate polymer interactions in the LbL films. This model indicates that there is no change in the additive volume mixing term, k, but a 3-fold increase in the heterogeneous specific interaction term, q, near the free surface. It has been discussed elsewhere[62] that deviations from additivity for physical properties of blends such as density, free volume, and permeability are the result of segmental conformations and chain packing. We postulate that the mechanism responsible for the distance over which the heterogeneous chain packing extends into the film with the mechanism responsible for wave-assisted particle resuspension, deposition, and compaction, suggesting that a process similar to sedimentation occurs for the solution adsorption protocol used in LbL film assembly. Resuspension allows greater porosity and greater heterogeneity near the free surface while the underlying material is consolidated. The films in Figure 1b range in thickness from 85 to 560 nm, so additional data at fixed percentage through the thickness are also plotted in Figure 1b for 50%, 60%, and 70% of the distance to the substrate. The change from S-shaped behavior occurs at approximately 60% of the thickness. There are a number of reports on the properties of consolidating sediments and the sedimentation of charge-stabilized colloidal suspensions.[63−67] Owen[64] found that mud density was constant through the upper two-thirds of the bed but increased rapidly near the basal layer where the flocs had been rearranged and compressed.

There are several studies that suggest a densified layer at the substrate for LbL films,[56,68−72] which might be expected to be reflected in the free volume characteristics. Hübsch et al.[56] and Salomäki et al.[70] proposed a model for LbL film growth that allows film restructuring (a densification near the substrate) forbidding polyelectrolyte diffusion over that part of the film. At least one of the polyelectrolytes can diffuse into the entire film during each deposition step until a combination of the progressive densification near the substrate and the diffusion-limited depth of polyelectrolyte penetration establishes the limit of penetration. Porcel et al.[71] examined the effect of the dipping method versus spraying method on LbL film growth rate. Using film thickness as a function of number of pairs of layers as a guide, it was determined that the transition from exponential growth to linear growth takes place at about 10−12 deposition steps (10−12 bilayers). The thickness per bilayer depends on the polyelectrolyte parameters with weak polyelectrolytes forming thicker layers than strong polyelectrolytes. This transition is not dependent on having intermediate drying steps, is not a strong function of deposition technique (spraying versus dipping), and is not a strong function of spraying time or spraying rate. Although the results do not prove that the crossover from exponential to linear growth regime is due to a densification near the substrate that forbids diffusion of polyelectrolyte in that region, all of the results are consistent with this model.

The blends were further examined using PAS. These particular blend samples are different from those measured by DBES (see Table 1); indeed, three separate sets of blends with differing layer number and preparation approach (mechanical vs manual) were prepared and measured. One set was measured by DBES, and the other two sets were measured by PAS. Figure 2A and B shows the oPs intensity and lifetime data, respectively, for the blends as functions of implantation energy. The corresponding depth of implantation is shown on the secondary *x*-axis, and the film thickness as measured by ellipsometry is also marked. The oPs intensity data (Figure 3a) indicate that the concentration of free volume is greater near the free surface than near the substrate, confirming the Doppler *S* parameter results. These results have been modeled by the interaction parameter model (eq 1) to confirm the increased level (1.5-fold increase) of heterogeneous specific interactions near the free surface. The oPs lifetime data do not vary as a

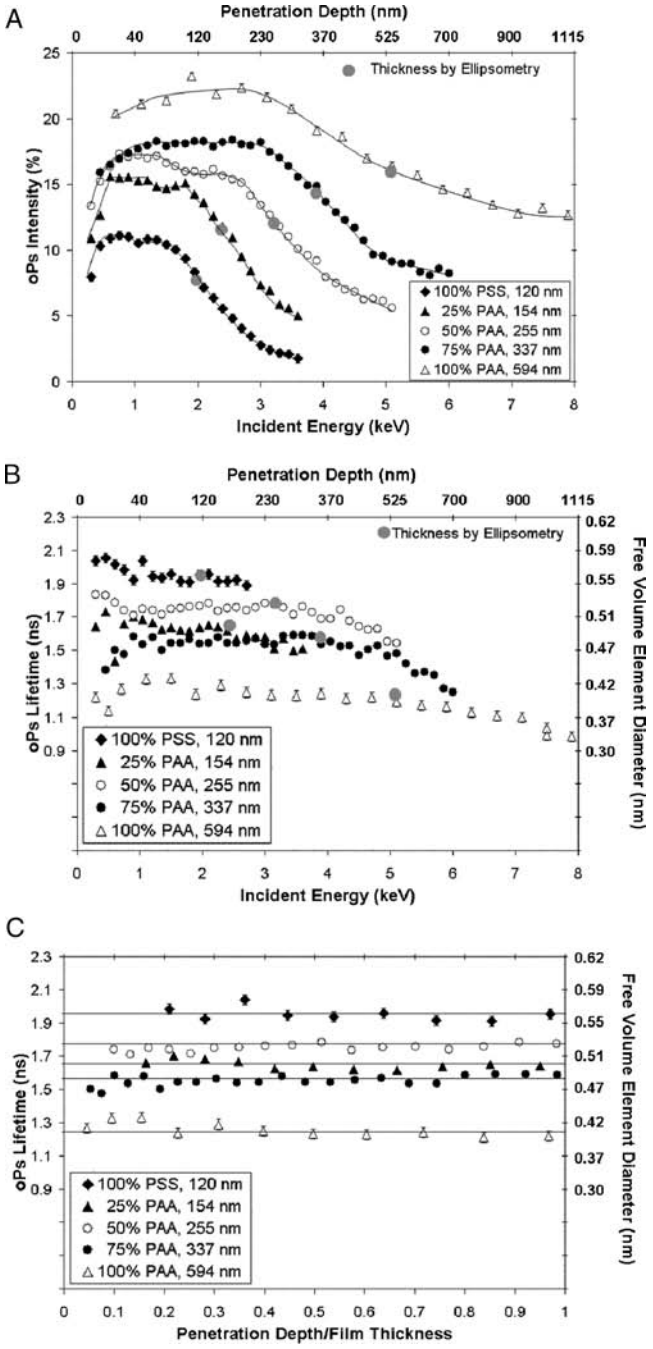

Figure 2. (A) PAS parameter oPs intensity as a function of blend composition and implantation energy. (B) PAS parameter oPs lifetime and free volume size as a function of blend composition and implantation energy. (C) PAS parameter oPs lifetime and free volume size as a function of normalized film thickness for films of composition PSS/PAH and PAA/PAH and their blends.

function of implantation depth (Figure 2B), and therefore they can be presented as a function of penetration depth normalized by film thickness as shown in Figure 2C. Figure 3b includes oPs lifetime data from the two blend series, one prepared by automated deposition of 20 bilayers and one prepared by manual dipping of 10 bilayers (Table 1). There is no appreciable effect of layer number, and hence thickness, on the oPs lifetime for these blends, nor is there a difference in average free volume element size for films prepared by automated or manual deposition. As such, it is evident that while the method of deposition does have some bearing on the thickness of the films prepared (see Table 1), there is little impact on the nanoscale material properties, at least as far as free volume element size is concerned. Figure 3b shows that the average free volume element size varies with blend composition from 4 to 6 Å. The oPs lifetime shows S-shaped behavior indicative of heterogeneity in polymer blends and shows this heterogeneity throughout the thickness of the films. Average free volume element size does not display a gradient from the free surface to the substrate; therefore, is the concentration of free volume elements (derived from both *S* parameter and oPs intensity data), but not their average size (derived from oPs lifetime data), the supporting evidence for a variation in chain packing across the film thickness due to adsorption-assisted sedimentation? The question arises as to whether a certain minimum thickness is required for consolidation to occur. This thickness will be composition dependent and can be established by examining films of identical composition and varying thickness; this will be presented and discussed in the next section.

Figure 2C is a convenient way to compare the trends in oPs lifetime data for films of varying thickness and will be used in subsequent figures. As discussed by Kobayashi et al.,[28] the mean oPs lifetime is the best fit of a discrete sum of decaying exponentials to the timing histogram data. The fitting program also gives a standard deviation on the lifetime as an indication of goodness of fit. Escape to vacuum of oPs formed in the near-surface region makes it difficult to reliably fit the data, giving a higher standard deviation for fits near the free surface. Figure 4 displays the values for oPs lifetime and standard deviation as a function of implantation energy for three LbL films of varying composition and thickness. The variation in standard deviation near the free surface can be used to determine a minimum depth of approximately 17 nm for extraction of reliable oPs lifetimes and free volume element sizes in these thin films. Figure 4 also shows that the standard deviation increases when the positrons are being implanted into the silicon substrate, giving a measure of the film thickness that compares well with that from ellipsometry.

Number of Bilayers. As shown in Table 1, two sets of films were prepared with the same preparation methodology and chemical composition but varying number of bilayers. Both sets were composed of strong polyelectrolytes. Figure 5a and b shows data for films prepared from PAH adsorbed in alternation with a blend of 90% PSS and 10% PAA, with bilayer number varying from 10 to 60, resulting in film thicknesses varying from approximately 50 to 600 nm. The oPs lifetime data in Figure 5a do not show a systematic variation with either film thickness or depth through the film. The thinnest film of 10 bilayers and approximately 50 nm thickness has a longer oPs lifetime than the 15−60 bilayer films. The average free volume element size for each of the films is 0.57, 0.52, 0.52, 0.54, and 0.54 nm as bilayer number increases from 10 to 60. Population standard deviations for each data set are used as error bars in Figure 5a. The oPs intensity data in Figure 5b will be further discussed after presentation of the second series of films of varying thickness composed of PAH/PSS bilayers. Data for films composed of PAH adsorbed in alternation with PSS are shown in Figure 6a and b. The oPs lifetime data in Figure 6a do not show a systematic variation with either film thickness or depth through the film. One of these films was prepared with lower salt concentration (0.1 M as compared to 0.5 M for the other three films), and the oPs

dx.doi.org/10.1021/ja308716v | J. Am. Chem. Soc. 2012, 134, 19808−19819

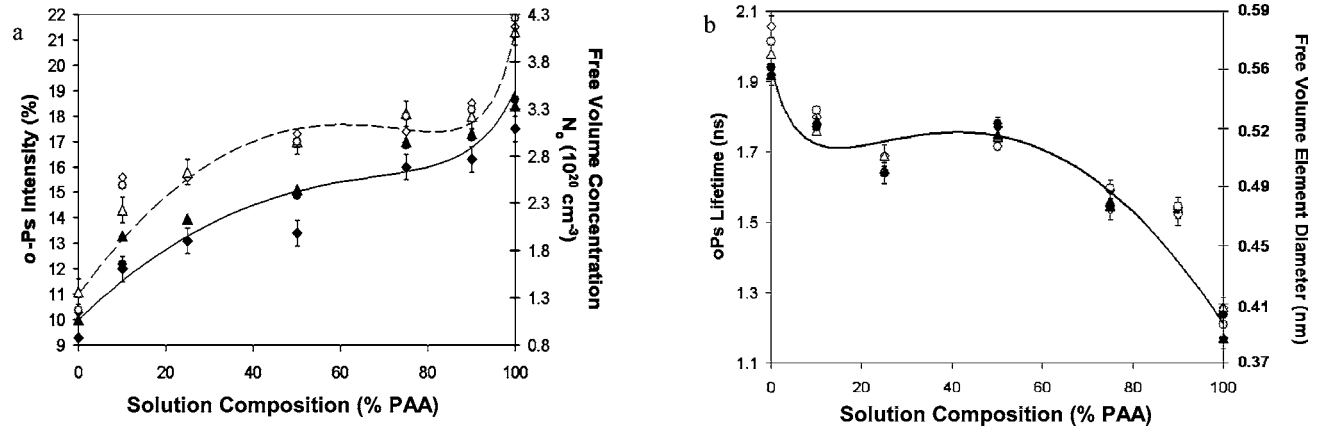

Figure 3. (a) PAS oPs intensity data and free volume concentration as a function of adsorption solution composition and depth. Circles correspond to the 10-layer samples deposited by hand for a distance 15% of the total thickness from the free surface (open) or 15% from the substrate (closed). The diamonds and triangles correspond to the 20 layer automatically deposited samples. The diamonds are for 10% of the total film thickness from free surface (open) or 10% from substrate (closed), while the triangles are for 20% from free surface (open) or 20% from substrate (closed). Lines are Kwei interaction parameter fits[60] (k = 10.72 and q increases from 15 to 22.5 to accurately model near-substrate versus near-free surface data, respectively). (b) oPs lifetime and free volume element size as functions of blend composition. Circles correspond to the 10-layer samples deposited by hand for a distance 15% of the total thickness from the free surface (open) or 15% from the substrate (closed). The diamonds and triangles correspond to the 20-layer automatically deposited samples. The diamonds are for 10% of the total film thickness from free surface (open) or 10% from substrate (closed), while the triangles are for 20% from free surface (open) or 20% from substrate (closed). Line is fit to Kwei interaction parameter model[60] with k = 0.1 and q = 0.45.

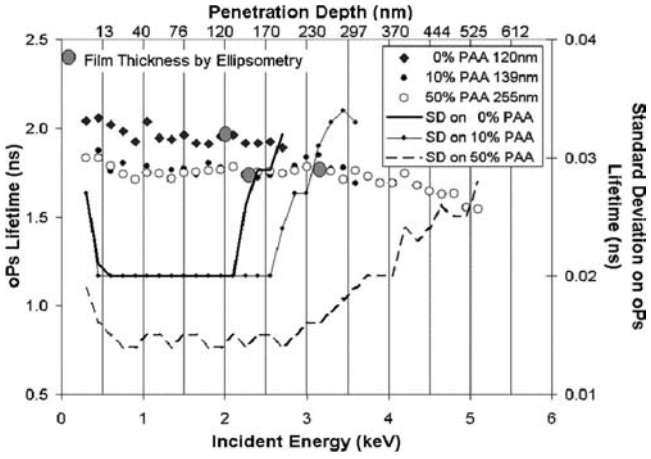

Figure 4. PAS parameter oPs lifetime and standard deviation on oPs lifetime as functions of implantation energy and penetration depth for three compositions of films of different thickness.

lifetime data are slightly larger for this film, a result that will be further discussed in the subsequent section entitled "Salt". These films range in thickness from approximately 80 to 240 nm. The results in Figures 5a and 6a indicate unambiguously that there is no lateral variation in the size of free volume elements in the films. The oPs intensity data for both series of films (Figures 5b and 6b) are plotted in Figure 7 to examine trends in the free volume concentration in films of the same composition but varying thickness to further quantify the regions of stratification through the film depth. Films of thickness <250 nm show less and less near-substrate compaction as film thickness decreases, to the point where a 50 nm film has no gradient; that is, the near-surface and near-substrate chain packing as measured by free volume concentration are identical. These results are similar in form to measured density profiles for sedimentation,[67] and support the lack of observation[71] of compacted substrate layers in LbL films made from strong polyelectrolytes with thicknesses less than 50 nm.

Some methods of preparing ultrathin polymer films of glassy homopolymers from solution, such as polystyrene[73] and polysulfone,[32] use different concentrations of polymer in solution to form films of varying thickness by spin-casting. It has been suggested that the variation in free volume properties between ultrathin films and thicker films could be due to variation in chain entanglement because of variations in solution concentrations.[73] One important point in our work on LbL films is that films (from 50 to 600 nm) have been prepared using the same solution concentration by varying the number of depositions; therefore, the results observed are not due to varying solution concentration.

Salt. The effect of the salt concentration on the assembly of LbL films from a variety of different polyelectrolytes has been widely studied.[50,74−76] There is evidence in the literature to suggest that a higher salt concentration leads to more effective complexation between the polyelectrolyte materials,[50,74] and to improved film stability.[75] It has been suggested that in polyelectrolyte solutions of low salt concentration the chains have an extended conformation as compared to high salt concentrations where the chains are globular due to charge screening.[69] This difference in conformation is postulated to cause thicker films when polyelectrolytes are adsorbed at high salt concentrations in addition to larger amounts of polyelectrolyte being adsorbed per bilayer.[69] PAS was used to investigate the free volume of films that were assembled in the presence of varying concentrations of NaCl. Figure 8a and b shows the oPs lifetime and intensity results, respectively, for five LbL samples prepared from PAH and PSS deposited with different [NaCl] in the adsorbing solution (see Table 1). These films range in thickness from approximately 50 to 300 nm. Figure 8a shows that the films deposited with lower [NaCl] have longer oPs lifetimes than the films deposited at higher salt concentration. This result suggests that the higher [NaCl] leads to smaller free volume element sizes and explains the slightly

dx.doi.org/10.1021/ja308716v | J. Am. Chem. Soc. 2012, 134, 19808−19819

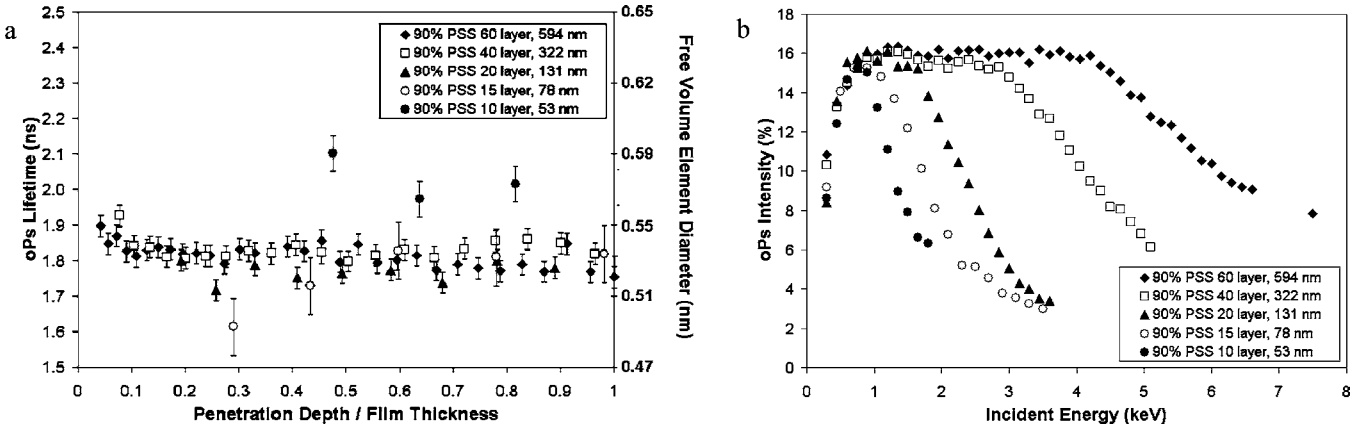

Figure 5. (a) PAS parameter oPs lifetime and free volume size as a function of normalized film thickness for films of constant composition PAH/90%PSS/10%PAA but varying thickness. The number of bilayer depositions is the only variable. (b) PAS parameter oPs intensity as a function of implantation energy for films of constant composition PAH/90%PSS/10%PAA but varying thickness. The number of bilayer depositions is the only variable.

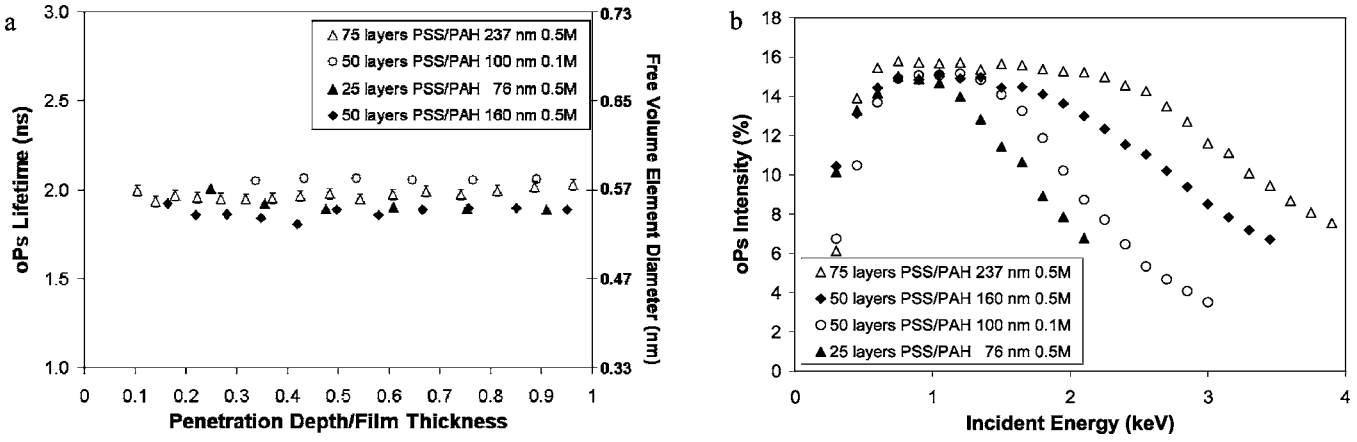

Figure 6. (a) oPs lifetime data and free volume size for films of identical composition, PSS/PAH, but varying thickness. The number of layer depositions is the only variable, except that one film is prepared with 0.1 M NaCl. (b) oPs intensity data for films of identical composition, PSS/PAH, but varying thickness. The number of layer depositions is the only variable, except that one film is prepared with 0.1 M NaCl.

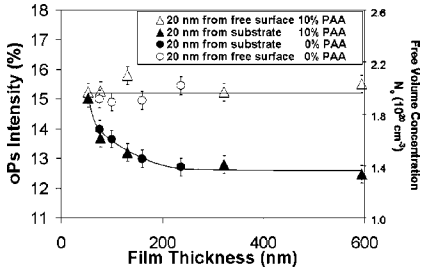

Figure 7. oPs intensity data for two series of films of varying thickness: 90%PSS/10%PAA (triangles) and 100%PSS/0%PAA (circles). The number of layer depositions is the only variable for the 90%PSS/10% PAA series, while layer number and salt concentration vary for the 100%PSS/0%PAA series. See Table 1 for details. Lines indicate trends.

higher oPs lifetime observed for the film prepared with lower salt concentration in Figure 6a. It is noted that this result does not correlate with the observed increase in film thickness with increasing salt concentration. It appears that the extended stiff conformation of polyelectrolytes adsorbed at low salt concentration leads to larger free volume element size in the film. Figure 8b shows that oPs intensity increases with higher salt concentration, suggesting that the enhancement in film thickness is at least partially due to an increase in the free volume concentration in the films. Thus, the altered conformation of the polyelectrolyte chains deposited at high salt concentrations not only causes higher amounts of polyelectrolyte in the bilayers and thicker films but also results in a greater free volume concentration in the films. This intriguing result suggests another method, in addition to blending and number of bilayers, for tailoring free volume in LbL films.

Molecular Weight. Literature shows that the molecular weight of the polymers used in LbL assembly can affect the final film properties, especially the film thickness, and to some extent the film stability.[7,77,78] Herein, studies were conducted to examine whether there was any effect on the free volume properties as a consequence of using polymers of markedly different molecular weights. Two systems were studied: hydrogen-bonded multilayers of poly(methacrylic acid) (PMA) with a weight average molecular weight (M_w) of 15 000 g mol^{-1} adsorbed in alternation with poly(vinyl pyrrolidone) (PVPON) with a M_w of 10 000 g mol^{-1}, and PMA of M_w of 100 000 g mol^{-1} adsorbed in alternation with PVPON with M_w of 360 000 g mol^{-1}. Both systems were assembled at a pH of 5.0 in acetate buffer with a final rinse in dilute HCl at pH 5.0 (see Table 1). Figure 9a and b gives the

dx.doi.org/10.1021/ja308716v | J. Am. Chem. Soc. 2012, 134, 19808−19819

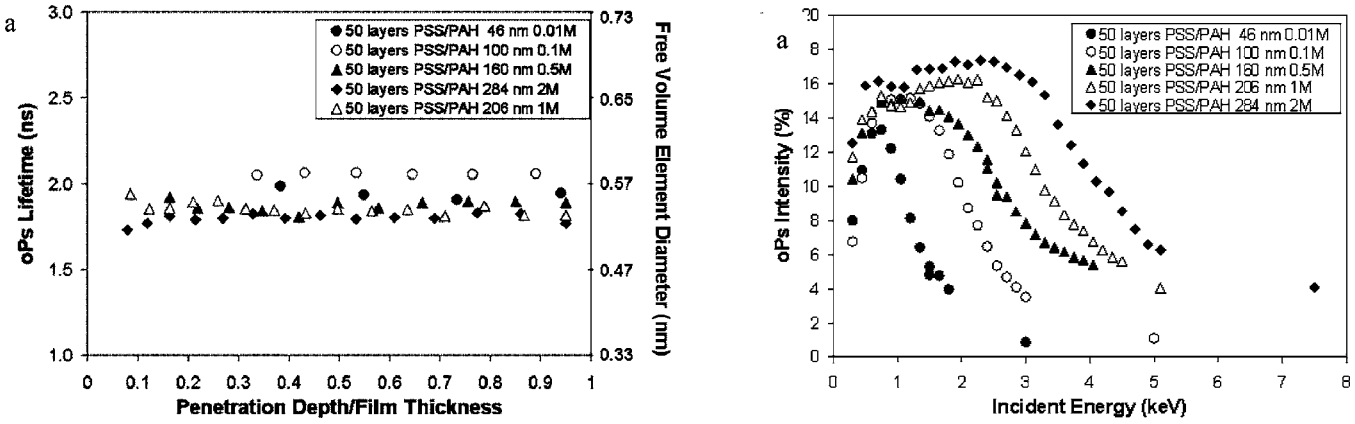

Figure 8. (a) oPs lifetime data and free volume size for films of identical layer number but varying salt concentration. (b) oPs intensity data for films of identical layer number but varying salt concentration.

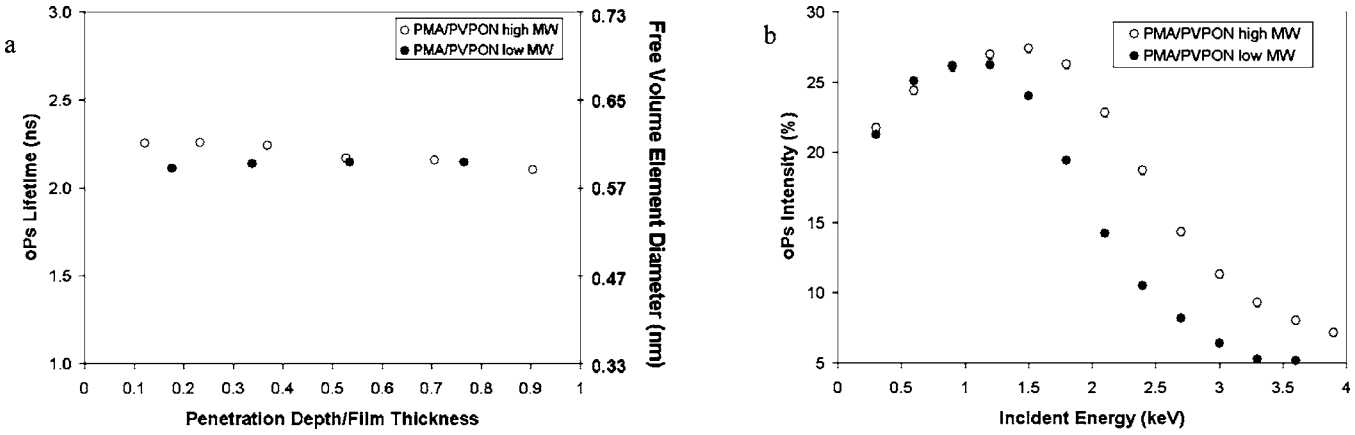

Figure 9. (a) oPs lifetime data and free volume size for films of varying molecular weight. (b) oPs intensity data for films of varying molecular weight.

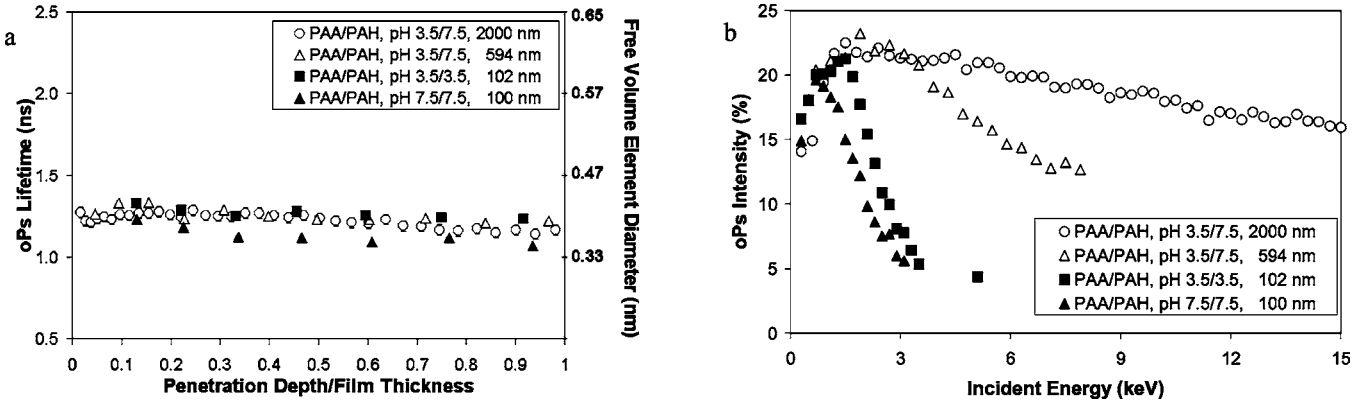

Figure 10. (a) oPs lifetime data and free volume size for films of varying pH of assembly (see Table 1). (b) oPs intensity data for films with varying pH of assembly (see Table 1).

oPs lifetime and intensity results, respectively, for the two LbL samples of (PMA/PVPON) multilayers, with the molecular weights (MW) denoted as "high" or "low". The low MW sample is thinner for the same number of bilayers (40 bilayers) and has a slightly lower oPs lifetime and intensity. There is not a large effect of molecular weight on the size and concentration of free volume elements in these LbL films. It is noted that this result may seem counterintuitive given that lower MW material may be expected to have more chain ends per unit volume and therefore more chain-end free volume per unit volume. These results, the first (to our knowledge) reported for hydrogen-bonded multilayers of varying MW, are contrary to what is typically observed for glassy polymers, which is that lower MW polymers have larger oPs lifetime and intensity.[79] Further systematic studies of MW effects in LbL films are warranted.

The results in Figure 9 are also significant in that they show the utility of PAS for investigating LbL films that are assembled using interactions other than electrostatics (in this case hydrogen bonding). Interestingly, the lifetime and intensity of the oPs embedded in the hydrogen-bonded multilayers is considerably larger than that of oPs embedded into any of the electrostatically bound systems investigated above. This result

dx.doi.org/10.1021/ja308716v | J. Am. Chem. Soc. 2012, 134, 19808−19819

suggests that there is considerably more free volume in the hydrogen-bonded systems investigated herein than in the electrostatic systems studied. While this result cannot necessarily be generalized to all hydrogen-bonded layers, it may be consistent with the fact that the 1:1 binding stoichiometry of charged sites expected in LbL films of electrostatic components is not necessarily expected in those constituted by hydrogen-bonding polymers. The resulting film structures may involve considerable loops and tails,[7] which may in turn result in a less dense structure with greater free volume.

Variation in Assembly pH. Weak polyelectrolytes have been used extensively in the preparation of multilayer films. The film properties depend on the pH of assembly[80] and postassembly variations in the environmental pH.[81] This responsiveness is attributed to groups in the polyelectrolyte structure being rendered uncharged by variations in the pH. Figure 10a and b shows the oPs lifetime and intensity results for four LbL samples prepared from PAA and PAH. In two cases, the polyelectrolytes were deposited (20 bilayers) at the same pH (either pH 7.5 or 3.5). In both of these cases, the rinses were performed at the same pH at which the layers were adsorbed. In the case where the assembly was performed entirely at pH 7.5, both polyelectrolytes are substantially charged in solution and in the final film.[72] As such, films assembled under these conditions are expected to behave similarly to strong polyelectrolytes. Conversely, in the scenario where the assembly is performed at pH 3.5, the PAH is highly charged with the primary amine groups being largely protonated, while the PAA is largely uncharged with most of the carboxylates protonated into carboxylic acid groups. These two films are compared to two films where the polyanion solution of PAA is adjusted to a pH of 3.5 and the PAH solution is prepared to pH 7.5. These two films differ only in the number of bilayers deposited, one having 10 bilayers and one having 20 bilayers. It can be seen from Figure 10a and b that the film deposited with PAA and PAH at pH 7.5 resulted in the thinnest film with slightly lower oPs lifetimes and intensities than the other films. Although this film tends toward chain packing similar to films assembled from strong polyelectrolytes (i.e., lower free volume concentration), the change is not substantial, especially when compared to the changes achieved by blending strong and weak polyelectrolytes (Figure 2A). In addition, the free volume element size also tends toward a smaller value. These results suggest that assembly pH can be used to alter the free volume properties of weak polyelectrolytes.

■ CONCLUSIONS

The greatest variation in free volume element size and concentration in LbL films was systematically achieved in this investigation through blending of PSS and PAA. The results have shown that it should be possible to target a particular free volume element size by using a particular proportion of PAA in the polyanion adsorption solution. These results indicate that a substantial change in free volume element diameter (2 Å) can be achieved by the introduction of a secondary polyelectrolyte in the polyanion solution. These results also suggest that blending of polyelectrolytes could be used to tailor free volume size for specific application of ultrathin LbL films as active layers for membranes based on size sieving separations, where the tightly defined free volume size can be utilized to control the transport of molecular and ionic species.[82] It is also evident that blending of PSS and PAA in the polyanion adsorption solution has a large effect on the concentration of free volume elements in the films, and these results provide evidence that the number of cavities can be tailored for controlled transport. While the present studies have utilized a blend of weak and strong polyelectrolytes, it is likely that other blended systems, such as blends of hydrogen bonding and electrostatic polymers,[83] or blends of inorganic particles and polymers,[84] will also allow tailoring of the free volume in thin film coatings.

The current study has also used a range of LbL film preparation variables and investigated their effect on the free volume in thin films. For those films assembled from strong polyelectrolytes, the number of bilayers was shown to have little effect on the free volume element size but rather a controlling effect on the lateral gradient in concentration of free volume. An increase in salt concentration of the adsorption solutions for films prepared from strong polyelectrolytes is shown to decrease individual void size while increasing the total free volume concentration. Hydrogen-bonded layered films show larger free volume element size and concentration than their electrostatically bonded counterparts. Variation in the solution pH of films prepared from weak polyelectrolytes is also shown to be a viable method to alter free volume characteristics of LbL thin films. These results give, for the first time, a clear indication of numerous methods to tailor the Ångström-scale free volume properties of LbL thin films by judicious selection of the assembly polymers and conditions. This level of control may allow tailoring of macromolecular transport properties through the films, which has implications for chemical separation, sensor, and storage/delivery applications of LbL films.

■ ASSOCIATED CONTENT

Supporting Information

Cross-sectional SEM images of LbL films. This material is available free of charge via the Internet at http://pubs.acs.org.

■ AUTHOR INFORMATION

Corresponding Author

fcaruso@unimelb.edu.au; anita.hill@csiro.au

Notes

The authors declare no competing financial interest.

■ ACKNOWLEDGMENTS

This work was supported by the Australian Research Council through the Discovery Project (F.C.) scheme. Additionally, support through the ARC Federation Fellowship scheme (F.C.), the ARC Australian Postdoctoral Fellowship scheme (S.J.P., J.F.Q.), and the CSIRO Science Leader Scheme (B.S., J.I.M., A.J.H.) is also gratefully acknowledged. The access to the major research facilities program is supported by the Commonwealth of Australia under the International Science Linkages program. Prof. Tim Bastow is thanked for assistance with data collection. Dr. Jiwei Cui and Joseph J. Richardson (The University of Melbourne) are thanked for assistance with the SEM measurements.

■ REFERENCES

(1) Merkel, T. C.; Freeman, B. D.; Spontak, R. J.; He, Z.; Pinnau, I.; Meakin, P.; Hill, A. J. *Science* **2002**, *296*, 519−522.

(2) Hiller, J.; Mendelsohn, J. D.; Rubner, M. F. *Nat. Mater.* **2002**, *1*, 59−63.

(3) Rusling, J. F.; Hvastkovs, E. G.; Hull, D. O.; Schenkman, J. B. *Chem. Commun.* **2008**, 141−154.

(4) Prime, K. L.; Whitesides, G. M. *J. Am. Chem. Soc.* **1993**, *115*, 10714−10721.
(5) Decher, G.; Hong, J.-D.; Schmitt, J. *Macromol. Chem., Macromol. Symp.* **1991**, *46*, 321−327.
(6) Decher, G. *Science* **1997**, *277*, 1232−1237.
(7) Stockton, W. B.; Rubner, M. F. *Macromolecules* **1997**, *30*, 2717−2725.
(8) Wang, L.; Wang, Z. Q.; Zhang, X.; Shen, J. C.; Chi, L. F.; Fuchs, H. *Macromol. Rapid Commun.* **1997**, *18*, 509−514.
(9) Lvov, Y.; Ariga, K.; Ichinose, I.; Kunitake, T. *Thin Solid Films* **1996**, *284/285*, 797−801.
(10) Ferreira, M.; Fiorito, P. A.; Oliveira, O. N., Jr.; Cordoba de Torresi, S. I. *Biosens. Bioelectron.* **2004**, *19*, 1611−1615.
(11) Lvov, Y.; Decher, G.; Sukhorukov, G. B. *Macromolecules* **1993**, *26*, 5396−5399.
(12) Caruso, F.; Spasova, M.; Saigueirino-Maceira, V.; Liz-Marzan, L. *Adv. Mater.* **2001**, *13*, 1090−1094.
(13) Ostrander, J. W.; Mamedov, A. A.; Kotov, N. A. *J. Am. Chem. Soc.* **2001**, *123*, 1101−1110.
(14) Johnston, A. P. R.; Read, E. S.; Caruso, F. *Nano Lett.* **2005**, *5*, 953−956.
(15) Yang, S. Y.; Lee, D.; Cohen, R. E.; Rubner, M. F. *Langmuir* **2004**, *20*, 5978−5981.
(16) Ruths, J.; Essler, F.; Decher, G.; Riegler, H. *Langmuir* **2000**, *16*, 8871−8878.
(17) Poptoshev, E.; Schoeler, B.; Caruso, F. *Langmuir* **2004**, *20*, 829−834.
(18) Ngankam, A. P.; Van Tassel, P. R. *Langmuir* **2005**, *21*, 5865−5871.
(19) Lvov, Y.; Ariga, K.; Ichinose, I.; Kunitake, T. *J. Am. Chem. Soc.* **1995**, *117*, 6117−6123.
(20) Lvov, Y.; Ariga, K.; Onda, M.; Ichinose, I.; Kunitake, T. *Langmuir* **1997**, *13*, 6195−6203.
(21) Kidambi, S.; Bruening, M. L. *Chem. Mater.* **2005**, *17*, 301−307.
(22) Jaber, J. A.; Schlenoff, J. B. *Chem. Mater.* **2006**, *18*, 5768−5773.
(23) Jaber, J. A.; Schlenoff, J. B. *J. Am. Chem. Soc.* **2006**, *128*, 2940−2947.
(24) Lutkenhaus, J.; Hrabak, K. D.; McEnnis, K.; Hammond, P. T. *J. Am. Chem. Soc.* **2005**, *127*, 17228−17234.
(25) Schwinte, P.; Voegel, J. C.; Picart, C.; Haikel, Y.; Schaaf, P.; Szalontai, B. *J. Phys. Chem. B* **2001**, *105*, 11906−11916.
(26) Smith, R. N.; McCormick, M.; Barrett, C. J.; Reven, L.; Spiess, H. W. *Macromolecules* **2004**, *37*, 4830−4838.
(27) Smith, R. N.; Reven, L.; Barrett, C. J. *Macromolecules* **2003**, *36*, 1876−1881.
(28) Kobayashi, Y.; Ito, K.; Oka, T.; He, C.; Mohamed, H. F. M.; Suzuki, R.; Ohdaira, T. *Appl. Surf. Sci.* **2008**, *255*, 174−178.
(29) Zubiaga, A; Garcia, J. A.; Plazaola, F.; Tuomisto, F.; Zuniga-Perez, J.; Munoz-Sanjose, V. *Phys. Rev. B* **2007**, *75*, 205305.
(30) Suzuki, R.; Mikado, T.; Chiwaki, M.; Ohgaki, H.; Yamazaki, T. *Appl. Surf. Sci.* **1995**, *85*, 87−91.
(31) Park, H. B.; Jung, C. H.; Lee, Y. M.; Hill, A. J.; Pas, S. J.; Mudie, S. T.; van Wagner, E.; Freeman, B. D.; Cookson, D. J. *Science* **2007**, *318*, 254−258.
(32) Rowe, B. W.; Pas, S. J.; Hill, A. J.; Suzuki, R.; Freeman, B. D.; Paul, D. R. *Polymer* **2009**, *50*, 6149−6156.
(33) Chen, Z.; Ito, K.; Yanagishita, H.; Oshima, N.; Suzuki, R.; Kobayashi, Y. *J. Phys. Chem. C* **2011**, *115*, 18055−18060.
(34) Bamford, D.; Dlubek, G.; Reiche, A.; Alam, M. A.; Meyer, W.; Galvosas, P.; Rittig, F. *J. Chem. Phys.* **2001**, *115*, 7260−7270.
(35) Hao, W. C.; Pan, F.; Wang, T. M.; Zhou, C. L.; Wei, L. *Chin. Phys. Lett.* **2006**, *23*, 223−226.
(36) Schönhoff, M.; Ball, V.; Bausch, A.; Dejugnat, C.; Delorme, N.; Glinel, K.; von Klitzing, R.; Steitz, R. *Colloids Surf., A* **2007**, *303*, 14−29.
(37) Vaca Chavez, F.; Schönhoff, M. *J. Chem. Phys.* **2007**, *126*, 104705.
(38) Liu, X.; Bruening, M. L. *Chem. Mater.* **2004**, *16*, 351−357.
(39) Jin, W.; Toutianoush, A.; Tieke, B. *Appl. Surf. Sci.* **2005**, *246*, 444−450.
(40) Wende, C.; Schönhoff, M. *Langmuir* **2010**, *26*, 8352−8357.
(41) Dubas, S. T.; Farhat, T.; Schlenoff, J. B. *J. Am. Chem. Soc.* **2001**, *123*, 5368−5369.
(42) Schlenoff, J. B.; Farhat, T. *Langmuir* **2001**, *17*, 1184−1192.
(43) Coffey, P. D.; Swann, M. J.; Waigh, T. A.; Schedin, F.; Lu, J. R. *Opt. Express* **2009**, *17*, 10959−10969.
(44) Tao, S. J. *J. Chem. Phys.* **1972**, *56*, 5499−5510.
(45) Eldrup, M.; Lightbody, D.; Sherwood, J. N. *Chem. Phys.* **1981**, *63*, 51−58.
(46) Hirata, K.; Kobayashi, Y.; Ujihira, Y. *J. Chem. Soc., Faraday Trans.* **1996**, *92*, 985.
(47) Sato, K.; Ito, K.; Hirata, K.; Yu, S.; Kobayashi, Y. *Phys. Rev. B* **2007**, *71*, 012201 1−4.
(48) Baker, J. A.; Chilton, N. B.; Coleman, P. G. *Appl. Phys. Lett.* **1991**, *59*, 164−166.
(49) Algers, J.; Sperr, P.; Egger, W.; Kögel, G.; Maurer, F. H. J. *Phys. Rev. B* **2003**, *67*, 125404.
(50) Losche, M.; Schmitt, J.; Decher, G.; Bouwman, W.; Kjaer, K. *Macromolecules* **1998**, *31*, 8893−8906.
(51) Sui, Z.; Schlenoff, J. B. *Langmuir* **2004**, *20*, 6026−6031.
(52) Quinn, J. F.; Yeo, J. C. C.; Caruso, F. *Macromolecules* **2004**, *37*, 6537−6543.
(53) Quinn, A.; Tjipto, E.; Yu, A. M.; Gengenbach, T. R.; Caruso, F. *Langmuir* **2007**, *23*, 4944−4949.
(54) Cho, J.; Quinn, J. F.; Caruso, F. *J. Am. Chem. Soc.* **2004**, *126*, 2270−2271.
(55) Debreczeny, M.; Ball, V.; Boulmedais, F.; Szalontai, B.; Voegel, J.-C.; Schaaf, P. *J. Phys. Chem. B* **2003**, *107*, 12734−12739.
(56) Hubsch, E.; Ball, V.; Senger, B.; Decher, G.; Voegel, J.-C.; Schaaf, P. *Langmuir* **2004**, *20*, 1980−1985.
(57) Yap, H. P.; Quinn, J. F.; Ng, S. M.; Cho, J.; Caruso, F. *Langmuir* **2005**, *21*, 4328−4333.
(58) Yap, H. P.; Quinn, J. F.; Johnston, A. P. R.; Caruso, F. *Macromolecules* **2007**, *40*, 7581−7589.
(59) Chu, E. Y.; Pearce, E. M.; Kwei, T. K.; Yeh, T. F.; Okamoto, Y. *Makromol Chem. Rapid Commun.* **1991**, *12*, 1−4.
(60) Kwei, T. K. *J. Polym. Sci., Part C: Polym. Lett.* **1984**, *22*, 307−313.
(61) Lei, J.; Pearce, E. M.; Kwei, T. K.; Hamilton, W. A.; Smith, G. S.; Kwei, G. H. *Macromolecules* **1992**, *25*, 6770−6774.
(62) Liu, R. Y. F.; Bernal-Lara, T. E.; Hiltner, A.; Baer, E. *Macromolecules* **2004**, *37*, 6972−6979.
(63) Segré, P. N.; Liu, F.; Umbanhowar, P.; Weitz, D. A. *Nature* **2000**, *409*, 594−597.
(64) Owen, M. W. Hydraulics Research Station Report INT 83, Wallingford, England, 1970.
(65) Vanderborght, J.-P.; Wollast, R.; Billen, G. *Limnol. Oceanogr.* **1977**, *22*, 787−793.
(66) Hawley, N. *Geo-Mar. Lett.* **1981**, *1*, 7−10.
(67) Torfs, H.; Williamson, H.; Huysentruyt, H.; Toorman, E. *Coastal Eng.* **1996**, *29*, 27−45.
(68) Schmitt, J.; Grünewald, T.; Decher, G.; Pershan, P. S.; Kjaer, K.; Lösche, M. *Macromolecules* **1993**, *26*, 7058−7063.
(69) Ladam, G.; Schaad, P.; Voegel, J. C.; Schaaf, P.; Decher, G.; Cuisinier, F. *Langmuir* **2000**, *16*, 1249−1255.
(70) Salomäki, M.; Vinokurov, I. A.; Kankare, J. *Langmuir* **2005**, *21*, 11232−11240.
(71) Porcel, C.; Lavalle, P.; Ball, V.; Decher, G.; Senger, B.; Voegel, J. C.; Schaff, P. *Langmuir* **2006**, *22*, 4376−4383.
(72) Choi, J.; Rubner, M. F. *Macromolecules* **2005**, *38*, 116−124.
(73) Ata, S.; Muramatsu, M; Takeda, J.; Ohdaira, T.; Suzuki, R.; Ito, K.; Kobayashi, Y.; Ougizawa, T. *Polymer* **2009**, *50*, 3343−3346.
(74) Dubas, S. T.; Schlenoff, J. B. *Langmuir* **2001**, *17*, 7725−7727.
(75) Tjipto, E.; Quinn, J. F.; Caruso, F. *Langmuir* **2005**, *21*, 8785−8792.
(76) Dubas, S. T.; Schlenoff, J. B. *Macromolecules* **1999**, *32*, 8153−8160.

(77) Sui, Z. J.; Salloum, D.; Schlenoff, J. B. *Langmuir* **2003**, *19*, 2491−2495.
(78) Guan, Y.; Yang, S.; Zhang, Y.; Xu, J.; Han, C. C.; Kotov, N. A. *J. Phys. Chem. B* **2006**, *110*, 13484−13490.
(79) Yu, Z.; Yashi, U.; McGervey, J. D.; Jamieson, A. M.; Simha, R. *J. Polym. Sci., Part B* **1994**, *32*, 2637−2644.
(80) Shiratori, S. S.; Rubner, M. F. *Macromolecules* **2000**, *33*, 4213−4219.
(81) Mendelsohn, J. D.; Barrett, C. J.; Chan, V. V.; Pal, A. J.; Mayes, A. M.; Rubner, M. F. *Langmuir* **2000**, *16*, 5017−5023.
(82) Hammond, P. T. *Adv. Mater.* **2004**, *16*, 1271−1293.
(83) Li, Q.; Quinn, J. F.; Caruso, F. *Adv. Mater.* **2005**, *17*, 2058−2062.
(84) Li, Q.; Quinn, J. F.; Wang, Y.; Caruso, F. *Chem. Mater.* **2006**, *18*, 5480−5485.